

Chloroquine urea derivatives: synthesis and antitumor activity in vitro

Pavić, Kristina; Rajić, Zrinka; Mlinarić, Zvonimir; Uzelac, Lidija; Kralj, Marijeta; Zorc, Branka

Source / Izvornik: **Acta Pharmaceutica**, 2018, 68, 471 - 483

Journal article, Published version

Rad u časopisu, Objavljena verzija rada (izdavačev PDF)

<https://doi.org/10.2478/acph-2018-0039>

Permanent link / Trajna poveznica: <https://urn.nsk.hr/urn:nbn:hr:163:361119>

Rights / Prava: [In copyright](#)/[Zaštićeno autorskim pravom.](#)

Download date / Datum preuzimanja: **2024-09-14**



Repository / Repozitorij:

[Repository of Faculty of Pharmacy and Biochemistry University of Zagreb](#)



Chloroquine urea derivatives: synthesis and antitumor activity *in vitro*

KRISTINA PAVIĆ¹
ZRINKA RAJIĆ¹
ZVONIMIR MLINARIĆ¹
LIDIJA UZELAC²
MARIJETA KRALJ²
BRANKA ZORC¹

¹ University of Zagreb
Faculty of Pharmacy and Biochemistry
Department of Medicinal Chemistry
HR-10 000 Zagreb, Croatia

² Rudjer Bošković Institute
Division of Molecular Medicine
Laboratory of Experimental Therapy
HR-10 000 Zagreb, Croatia

Accepted September 11, 2018
Published online September 14, 2018

In the current paper, we describe the design, synthesis and antiproliferative screening of novel chloroquine derivatives with a quinoline core linked to a hydroxy or halogen amine through a flexible aminobutyl chain and urea spacer. Synthetic pathway leading to chloroquine urea derivatives 4–10 includes two crucial steps: *i*) synthesis of chloroquine benzotriazolide 3 and *ii*) formation of urea derivatives through the reaction of compound 3 with the corresponding amine. Testing of antiproliferative activity against four human cancer cell lines revealed that chloroquine urea derivatives 9 and 10 with aromatic moieties show activity at micromolar concentrations. Therefore, these molecules represent interesting lead compounds that might provide an insight into the design of new anticancer agents.

Keywords: chloroquine, hydroxychloroquine, urea, antitumor activity *in vitro*

Chloroquine and its related drug, hydroxychloroquine, are antimalarial agents active against the asexual form of *Plasmodium* inside red blood cells (1). They are members of the 4-substituted quinoline drug class, along with mefloquine, amodiaquine and the parent drug quinine. Chloroquine and hydroxychloroquine interfere with the biosynthesis of nucleic acids in *Plasmodium* and inhibit heme polymerase that converts toxic heme, a product of hemoglobin decomposition caused by a parasite, into non-toxic hemozoin, resulting in the accumulation of heme within the parasite (2). Anticancer properties of these drugs are also well documented; they affect the Toll-like receptor 9, p53 and CXCR4-CXCL12 pathway in cancer cells, tumor vasculature and immune system, augment TRAIL-induced apoptosis and induce G2/M phase arrest in human cancer cells (3, 4). Scientific evidence also supports the use of chloroquine and hydroxychloroquine in combination with conventional anticancer drugs (3, 5–8). Their chemosensitizing and radiosensitizing activities have been confirmed in over 30 clinical studies with different cancer types and in combination with various anticancer treatments. It has been confirmed that chloroquine and hydroxychloroquine inhibit autophagy, a cellular recycling system, involving lysosomal degradation that minimizes the production of reactive oxygen species related to tumor

* Correspondence; e-mail: bzorc@pharma.hr

reoxygenation and tumor exposure to chemotherapeutic agents and radiation (9–11). Targeting autophagy can overcome BRAF inhibitor resistance mechanisms in autophagy-dependent tumors, *e.g.*, in brain tumors. Mulcahy Levy *et al.* (12) reported successful treatment of a patient with chloroquine after failure of the BRAF^{V600E} inhibitor vemurafenib. However, organs in which autophagy plays a homeostatic role may be sensitive to the combined use of chloroquine and anticancer drugs (13).

Due to the above mentioned facts, derivatization of chloroquine has been in the focus of many researchers worldwide. Numerous chloroquine derivatives have been prepared in order to overcome *Plasmodium* resistance, the main problem in malaria treatment (see, for example, refs. 14–16) or in finding new anticancer agents (refs. 17–20). In this paper, we report on the design and synthesis of chloroquine derivatives with potential antiproliferative properties. Our novel compounds are composed of the quinoline core, aminobutyl chain and hydroxy or halogenamine moiety bound by the urea spacer. The rationale for the design of these compounds is supported by the fact that quinoline and amino alcohol pharmacophores are present in several antimalarial drugs (quinine, mefloquine, lumefantrine, halofantrine) (21), while urea motif is crucial in several kinase inhibitors, a subclass of antitumor agents (sorafenib, regorafenib) (22). The two here described compounds are organofluoro derivatives. It is known that approximately 20 % of currently approved drugs contain one or more fluorine atoms: fluoro derivatives have increased stability, selectivity and/or membrane permeability compared to their nonfluorinated analogs, so incorporation of fluorine in a drug candidate is a common strategy in drug design and development (23).

EXPERIMENTAL

General

Melting points were measured on a Stuart Melting Point (SMP3) apparatus (Barloworld Scientific, UK) in open capillaries with uncorrected values. A CEM Discover microwave reactor was used for microwave reactions (CEM GmbH, Germany). IR spectra were recorded on a Paragon 500 (PerkinElmer, UK) FT-IR spectrophotometer and UV-Vis spectra on a Lambda 20 double beam spectrophotometer (PerkinElmer). ¹H and ¹³C NMR spectra were recorded at 25 °C on an NMR Avance 600 spectrometer (Bruker, Germany). Chemical shifts (δ) are reported in parts per million (ppm) relative to tetramethylsilane in the ¹H spectra and to dimethyl sulfoxide (DMSO) residual peak as reference in the ¹³C spectra (39.52 ppm). Coupling constants (*J*) are reported in Hertz (Hz). Mass spectra were collected on an HPLC-MS/MS instrument (HPLC, Agilent Technologies 1200 Series; MS, Agilent Technologies 6410 Triple Quad, USA). Mass determination was realized using electron spray ionization (ESI) in positive mode. Elemental analyses were performed on a CHNS LECO analyzer (LECO Corporation, USA). All compounds were routinely checked by TLC with Merck silica gel 60F-254 glass plates using an appropriate mobile phase (Merck, Germany). Spots were visualized by short-wave UV light and iodine vapour. Column chromatography was performed on silica gel 60 (0.063–0.200 mm) as the stationary phase.

All chemicals and solvents were of analytical grade and were purchased from commercial sources. Triphosgene, butane-1,4-diamine, 4,7-dichloroquinoline, 4-(chlorophenyl)(phenyl)methanamine hydrochloride, triethylamine (TEA) and (3-(4,5-dimethylthiazol-

2-yl)-2,5-diphenyltetrazolium bromide (MTT) were purchased from Sigma-Aldrich (USA), (1-aminocyclopropyl)methanol hydrochloride, (1-aminocyclobutyl)methanol, (1*R*,3*S*)-3-aminocyclopentanol hydrochloride, 2-amino-4-fluorobutan-1-ol, 3-amino-1,1,1-trifluoropropan-2-ol hydrochloride from Enamine (Ukraine), while 4-(2-aminoethyl)phenol (tyramine) and benzotriazole were purchased from Alfa Aesar (Thermo Fisher Scientific, USA). Anhydrous solvents were dried and redistilled prior to use.

Syntheses

*N*¹-(7-chloroquinolin-4-yl)butane-1,4-diamine (**1**). – A mixture of 4,7-dichloroquinoline (0.396 g, 0.002 mol) and 1,4-diaminobutane (1.763 g, 0.02 mol) was stirred under microwave irradiation (300 W) at 95 °C. After 60 min, the reaction mixture was diluted with dichloromethane, extracted with 5 % NaOH (4 × 40 mL) and washed with water (2 × 40 mL). Organic layer was dried over anhydrous sodium sulfate, filtered and evaporated under reduced pressure to give 0.531 g (90 %) of white solid **1** (24).

1-Benzotriazole carboxylic acid chloride (*BtcCl*, **2**). – 1-Benzotriazole carboxylic acid chloride (**2**) was prepared from benzotriazole and triphosgene according to the previously published procedure (25).

N-{4-[(7-chloroquinolin-4-yl)amino]butyl}-1*H*-1,2,3-benzotriazole-1-carboxamide (**3**). – To a cold solution (0 °C) of *BtcCl* (0.363 g, 0.002 mol) and TEA (0.202 g, 0.002 mol) in dry toluene (5 mL), a suspension of compound **1** (0.5 g, 0.002 mol) in dry dioxane (8 mL) was added dropwise. The reaction mixture was stirred at room temperature for 1 h. Solvent was evaporated under reduced pressure. The crude product was purified by column chromatography (dichloromethane/methanol 9:1) and triturated with ether to give white solid **3** (0.663 g, 84 %).

1-{4-[(7-Chloroquinolin-4-yl)amino]butyl}-3-[1-(hydroxymethyl)cyclopropyl]urea (**4**). – A mixture of compound **3** (0.158 g, 0.0004 mol), (1-aminocyclopropyl)methanol hydrochloride (0.099 g, 0.0008 mol), TEA (0.162 g, 0.0016 mol) and sodium dithionite (0.002 g) in dichloromethane (2 mL) was stirred under microwave irradiation (300 W) at 65 °C. After 20 min, the solvent was evaporated under reduced pressure; the residue was dissolved in ethyl acetate and extracted with 5 % NaOH solution (3 × 15 mL) and water (2 × 15 mL). The product started to precipitate from the organic layer, which was then vacuum filtered. The organic layer was evaporated under reduced pressure and combined with the residue after filtration. The white solid (0.113 g, 78 %) was collected after trituration with ether.

1-{4-[(7-Chloroquinolin-4-yl)amino]butyl}-3-[1-(hydroxymethyl)cyclobutyl]urea (**5**). – A mixture of compound **3** (0.158 g, 0.0004 mol), (1-aminocyclobutyl)methanol (0.081 g, 0.0008 mol), TEA (0.081 g, 0.0008 mol) and sodium dithionite (0.002 g) in dichloromethane (2 mL) was stirred under microwave irradiation (300 W) at 65 °C. After 20 min, the solvent was evaporated under reduced pressure. The residue was dissolved in ethyl acetate and extracted with 5 % NaOH solution (3 × 15 mL) and water (2 × 15 mL), dried over anhydrous sodium sulfate and evaporated. The yellow solid (0.082 g, 54 %) was collected after trituration with ether.

1-{4-[(7-Chloroquinolin-4-yl)amino]butyl}-3-[(1*R*,3*S*)-3-hydroxycyclopentyl]urea (**6**). – A mixture of compound **3** (0.158 g, 0.0004 mol), (1*R*,3*S*)-3-aminocyclopentane-1-ol hydro-

chloride (0.110 g, 0.0008 mol), TEA (0.162 g, 0.0016 mol) and sodium dithionite (0.002 g) in dichloromethane (2 mL) was stirred under microwave irradiation (300 W) at 65 °C. After 30 min, the solvent was evaporated under reduced pressure. The residue was dissolved in ethyl acetate and extracted with 5 % NaOH solution (3 × 15 mL) and water (2 × 15 mL), dried over anhydrous sodium sulfate and evaporated. After purification by column chromatography (cyclohexane/ ethyl acetate/ methanol 1:1:0.75), yellow oil (0.102 g, 68 %) was obtained.

1-[4-[(7-Chloroquinolin-4-yl)amino]butyl]-3-(4-fluoro-1-hydroxybutan-2-yl)urea (7). – A mixture of compound 3 (0.158 g, 0.0004 mol), 2-amino-4-fluorobutane-1-ol (0.086 g, 0.0008 mol), TEA (0.081 g, 0.0008 mol) and sodium dithionite (0.002 g) in dichloromethane (2 mL) was stirred under microwave irradiation (300 W) at 65 °C. After 40 min, the solvent was evaporated under reduced pressure. After two consequent triturations with water and ether, a white solid was obtained (0.123 g, 80 %).

1-[4-[(7-Chloroquinolin-4-yl)amino]butyl]-3-(3,3,3-trifluoro-2-hydroxypropyl)urea (8). – A mixture of compound 3 (0.158 g, 0.0004 mol), 3-amino-1,1,1-trifluoropropane-2-ol hydrochloride (0.132 g, 0.0008 mol), TEA (0.162 g, 0.0016 mol) and sodium dithionite (0.002 g) in dichloromethane (2 mL) was stirred under microwave irradiation (300 W) at 65 °C. After 30 min, the solvent was evaporated under reduced pressure; the residue was dissolved in ethyl acetate and extracted with 5 % NaOH solution (3 × 15 mL) and water (2 × 15 mL), dried over anhydrous sodium sulfate and evaporated. The white solid (0.118 g, 73 %) was collected after trituration with ether.

1-[4-[(7-Chloroquinolin-4-yl)amino]butyl]-3-(4-hydroxyphenethyl)urea (9). – A mixture of compound 3 (0.158 g, 0.0004 mol), 4-(2-aminoethyl)phenol (0.110 g, 0.0008 mol), TEA (0.081 g, 0.0008 mol) and sodium dithionite (0.002 g) in dichloromethane (2 mL) was stirred under microwave irradiation (300 W) at 65 °C. After 40 min, the solvent was evaporated under reduced pressure. After purification by column chromatography (dichloromethane/methanol 9.5:0.5) and trituration with ether, a pale yellow solid (0.149 g, 90 %) was obtained.

1-[(4-Chlorophenyl)(phenyl)methyl]-3-[4-[(7-chloroquinolin-4-yl)amino]butyl]urea (10). – A mixture of compound 3 (0.158 g, 0.0004 mol), (4-chlorophenyl)(phenyl)methanamine hydrochloride (0.203 g, 0.0008 mol), TEA (0.162 g, 0.0016 mol) and sodium dithionite (0.002 g) in dichloromethane (2 mL) was stirred under microwave irradiation (300 W) at 65 °C. After 40 min, the solvent was evaporated under reduced pressure. The residue was dissolved in ethyl acetate and extracted with 5 % NaOH solution (3 × 15 mL). The product started to precipitate from the organic layer, which was then vacuum filtered. The organic layer was evaporated under reduced pressure and combined with the residue after filtration. The white solid (0.093 g, 47 %) was collected after trituration with ether.

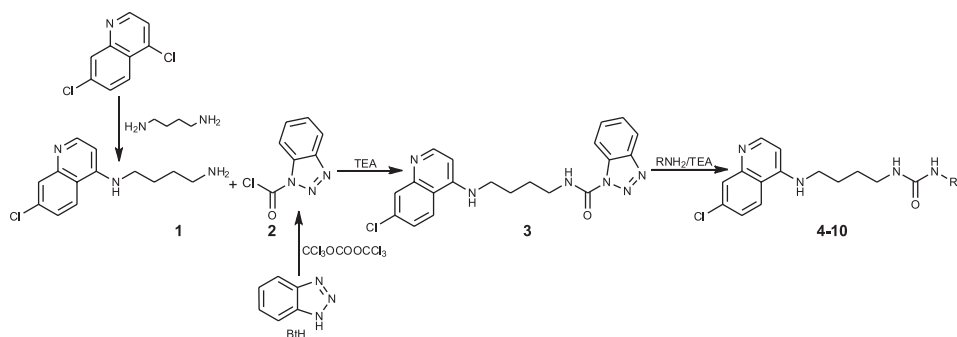
Cell viability assay

HCT 116 (colon carcinoma), MCF-7 (breast adenocarcinoma), H 460 (lung carcinoma) and SW 620 (colon carcinoma) cells (American Type Culture Collection, ATCC, USA) were cultured as monolayers and maintained in Dulbecco's modified Eagle medium (DMEM), supplemented with 10 % fetal bovine serum (FBS), 2 mmol L⁻¹ L-glutamine, 100 U mL⁻¹ penicillin and 100 µg mL⁻¹ streptomycin in a humidified atmosphere with 5 % CO₂ at 37 °C.

The growth inhibition activity was assessed as described previously (26, 27). Briefly, the cells were seeded into standard 96-well microtiter plates on day 0. Cell concentrations were adjusted according to the cell population doubling time (PDT): 3000 cells per well for HCT116 and SW 620 cell lines (PDT = 20–24 h) and 4,000 cells per well for MCF-7 cell lines (PDT = 33 h). Afterwards, the tested compounds were added into five consecutive 10-fold dilutions (10^{-8} to 10^{-4} mol L⁻¹) and incubated for further 72 h. Working dilutions were freshly prepared on the day of testing. The solvent (DMSO) was also tested for the possible inhibitory activity by adjusting its concentration to be the same as in working concentrations (maximum concentration of DMSO was 0.25 %). After 72 h of incubation, the cell growth rate was evaluated by performing the MTT assay that detects dehydrogenase activity in viable cells. The absorbance was measured on a microplate reader at 570 nm. Each test point was performed in quadruplicate in at least three individual experiments. The results are expressed as IC_{50} , which is the concentration necessary for 50 % of inhibition. The IC_{50} values for each compound were calculated from dose-response curves using linear regression analysis, using FORCAST function in Excel, by fitting the test concentrations that give PG (percentage of growth) values above and below the reference value (*i.e.*, 50 %). Each result is the mean value from three separate experiments.

RESULTS AND DISCUSSION

The novel chloroquine derivatives **4–10** were prepared by a simple two-step method, which includes synthesis of benzotriazolide **3** and its aminolysis with the corresponding amine: (1-aminocyclopropyl)methanol, (1-aminocyclobutyl)methanol, (1*R*, 3*S*)-3-aminocyclopentanol, 2-amino-4-fluorobutan-1-ol, 3-amino-1,1,1-trifluoropropan-2-ol, 4-(2-aminoethyl)phenol (tyramine) or 4-(chlorophenyl)(phenyl)methanamine). The following reaction step was carried out in a microwave reactor in the presence of TEA. Compound **3** was prepared by acylation of chloroquine derivative **1** with 1-benzotriazole carboxylic acid chloride (**2**), while the starting compounds **1** and **2** were prepared from commercially available 4,7-dichloroquinoline and butane-1,4-diamine (**24**), and benzotriazole and triphosgene (**25**), resp. The strategy for the preparation of the title compounds is given in Scheme 1.



Scheme 1

Purification of compounds was carried out using crystallization methods and/or column chromatography. Yields for urea derivatives **4–10** ranged from 47 to 90 %. Structures of new compounds **4–10** were confirmed by IR, ^1H and ^{13}C NMR spectra. All spectral data are given in Table I. Enumeration of atoms is presented in Fig. 1.

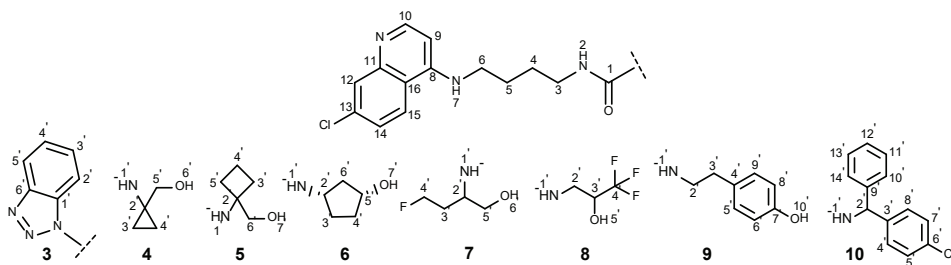


Fig. 1. Atom enumeration of compounds **3–10** in NMR spectra.

Quinoline hydrogen atoms at positions 10, 15, 12, 14 and 9 in ^1H NMR spectra appeared as doublets at δ 8.41–8.35, 8.35–8.26, 7.80–7.76, 7.49–7.40 and 6.54–6.45 ppm, resp. Two NH groups in the spacer at positions 2 and 7 appeared as triplets at δ 7.65–7.31 and 6.07–5.91 ppm, while the position of OH groups ranged from 6.15 and 3.45 ppm (all signals D_2O exchangeable). Quinoline carbon atoms in ^{13}C spectra were located in the aromatic region and gave the appropriate atom count. Carbonyl C-atom gave a signal between 158.84 and 157.21 ppm. In addition, the presence of a carbonyl functional group was indicated by the appearance of two strong stretching vibration bands in IR spectra at 1660–1613 and 1590–1579 cm^{-1} . The carbonyl group in benzotriazolide **3** was shifted to higher wavenumbers (1736 and 1577 cm^{-1}) and lower ppm values (149.02). The signal of carbon atom 2' in product **10** bearing two phenyl residues showed up at δ 6.88–6.85 ppm (doublet, ^1H NMR) and 56.26 ppm (^{13}C NMR), resp. Phenyl and benzhydryl residues in urea derivatives **9** and **10** gave the expected signals in the aromatic region and appropriate hydrogen/carbon count. Carbon atom 4' in urea **8** with three fluorine atoms and the neighboring atom 3' gave quartets with the coupling constants of 283.76 and 28.35 Hz, resp. Chemical structure of new compounds was also supported by CHN analysis and mass spectroscopy. Molecular ion peaks corresponding to the expected molecular formulas were obtained for all compounds. m/z data and the expected relative molecular masses are given in Table I, while NMR and mass spectra are collected in Supplementary Material.

Drug-like properties of novel CQ-derivatives were calculated using the Chemicalize.org program (28). A common set of physicochemical parameters was calculated: number of atoms, molecular weight (M_r), partition coefficient ($\log P$), number of H-bond donors (HBD), number of H-bond acceptors (HBA), molar refractivity (MR) and topological polar surface area (TPSA). These parameters are presented in Table II. All compounds (except compound **10**, which showed minimal aberration in $\log P$) are fully in agreement with Lipinski's and Gelovani's rules for prospective small molecular drugs (number of atoms 20–70, $M_r \leq 500$, $\log P \leq 5$, number of HBD ≤ 5 , number of HBA ≤ 10 , MR within the range of 40 and 130 $\text{cm}^3 \text{mol}^{-1}$, TPSA $< 140 \text{ \AA}^2$).

Table 1. Analytical and spectral data of compounds 3–10

Compd.	M. p. (°C)	IR (KBr, film), ν_{\max} (cm ⁻¹)	NMR data (DMSO- <i>d</i> ₆ , δ ppm)		MS (<i>m/z</i>)	Molecular formula (<i>M</i>)	CHN analysis, calcd./found (%)	
			¹ H	¹³ C				
3	190–192	3365, 3253, 3103, 3065, 3021, 2937, 2860, 1736, 1614, 1577, 1529, 1445, 1366, 1331, 1284, 1234, 1203, 1141, 1082, 1010, 941, 891, 853, 820, 754, 623, 536, 478	9.31–9.27 (t, <i>J</i> = 5.76 Hz, 1H, 2), 8.39–8.37 (d, <i>J</i> = 5.45 Hz, 1H, 10), 8.30–8.27 (d, <i>J</i> = 9.06 Hz, 1H, 15), 8.22–8.19 (d, <i>J</i> = 9.05 Hz, 2H, 2'), 131.33 (1'), 129.87 (3'), 127.15 (14), 125.47 (4), 124.15, 124.06 (12, 15), 119.74 (5'), 117.37 (16), 113.57 (2'), 98.65 (9), 42.06 (6), 39.72 (3), 26.55 (4), 25.07 (5)	151.53 (10), 150.26 (11), 149.02 (1), 148.96 (8), 145.45 (6'), 133.50 (13), 131.33 (1'), 129.87 (3'), 127.15 (14), 125.47 (4), 124.15, 124.06 (12, 15), 119.74 (5'), 117.37 (16), 113.57 (2'), 98.65 (9), 42.06 (6), 39.72 (3), 26.55 (4), 25.07 (5)	395.0 (M+1) ⁺	C ₂₀ H ₁₉ ClN ₃ O (394.13)	60.84 4.85 60.67 4.61	21.28 21.40
			3359, 2929, 2859, 1645, 1613, 1590, 1569, 1496, 1454, 1429, 1375, 1325, 1273, 1255, 1205, 1169, 1078, 1039, 904, 871, 853, 798, 768, 746, 643, 603, 573	8.39–8.37 (d, <i>J</i> = 5.42 Hz, 1H, 10), 8.31–8.28 (d, <i>J</i> = 9.05 Hz, 1H, 15), 7.77–7.76 (d, <i>J</i> = 2.21 Hz, 1H, 12), 7.45–7.41 (dd, <i>J</i> = 2.25, 8.99 Hz, 1H, 14), 7.38–7.34 (t, <i>J</i> = 5.25 Hz, 1H, 2), 6.48–6.46 (d, <i>J</i> = 5.48 Hz, 1H, 9), 6.41 (s, 1H, 1'), 6.12 (bs, 1H, 7), 4.95 (bs, 1H, 6'), 3.28–3.23 (m, 2H, 6, 5'), 3.07–3.00 (q, <i>J</i> = 6.54 Hz, 2H, 3), 1.67–1.62, 1.53–1.46 (2m, 4H, 4, 5), 0.65–0.51 (m, 4H, 3, 4)	158.84 (1), 151.92 (10), 150.08 (11), 149.12 (8), 133.31 (13), 127.47 (14), 124.15, 123.95 (12, 15), 117.47 (16), 98.64 (9), 66.19 (5'), 42.17 (6), 38.86 (3), 34.29 (2'), 27.69 (4), 25.15 (5), 11.62 (3', 4)	363.1 (M+1) ⁺	C ₁₈ H ₂₃ ClN ₄ O ₂ (362.85)	59.58 6.39 59.46 6.22
5	160 (decomp.)	3355, 2984, 2940, 2850, 1660, 1584, 1550, 1489, 1474, 1449, 1429, 1370, 1332, 1304, 1282, 1253, 1200, 1167, 1135, 1080, 1056, 1039, 908, 855, 824, 800, 769, 742, 676, 645, 601, 532	8.40–8.38 (d, <i>J</i> = 5.37 Hz, 1H, 10), 8.30–8.27 (d, <i>J</i> = 9.04 Hz, 1H, 15), 7.78–7.77 (d, <i>J</i> = 2.15 Hz, 1H, 12), 7.45–7.42 (dd, <i>J</i> = 2.18, 8.96 Hz, 1H, 14), 7.36–7.32 (t, <i>J</i> = 5.34 Hz, 1H, 2), 6.49–6.47 (d, <i>J</i> = 5.49 Hz, 1H, 9), 5.93 (m, 2H, 7, 1'), 5.03 (bs, 1H, 7'), 3.45 (s, 2H, 6'), 3.31–3.26 (m, 2H, 6), 3.06–2.99 (q, <i>J</i> = 6.44 Hz, 2H, 3), 2.17–2.07, 1.99–1.91, 1.76–1.63, 1.52–1.45 (4m, 10H, 4, 5, 3'-5')	157.80 (1), 151.92 (10), 150.07 (11), 149.12 (8), 133.33 (13), 127.48 (14), 124.11, 123.95 (12, 15), 117.46 (16), 98.65 (9), 66.13 (5'), 56.64 (2'), 42.17 (6), 38.65 (3), 29.55 (3', 5'), 27.77 (4), 25.21 (5), 13.95 (4)	377.1 (M+1) ⁺	C ₁₉ H ₂₅ ClN ₄ O ₂ (376.88)	60.55 6.69 60.57 6.61	14.87 14.76

Compd.	M. p. (°C)	IR (KBr, film), ν_{\max} (cm ⁻¹)	NMR data (DMSO- <i>d</i> ₆ , δ , ppm)		MS (<i>m/z</i>)	Molecular formula (<i>M_r</i>)	CHN analysis, calcd./found (%)
			¹ H	¹³ C			
6	oil	3323, 2932, 2861, 1642, 1584, 1451, 1369, 1334, 1281, 1254, 1207, 1138, 1082, 1030, 990, 853, 806, 767, 645, 428	8.40–8.38 (d, <i>J</i> = 5.44 Hz, 1H, 10), 8.31–8.28 (d, <i>J</i> = 9.08 Hz, 1H, 15), 7.78–7.77 (d, <i>J</i> = 2.20 Hz, 1H, 12), 7.46–7.42 (dd, <i>J</i> = 2.23, 8.99 Hz, 1H, 14), 7.40–7.36 (t, <i>J</i> = 5.10 Hz, 1H, 2), 6.49–6.47 (d, <i>J</i> = 5.51 Hz, 1H, 9), 5.91–5.87 (t, <i>J</i> = 5.69 Hz, 1H, 7), 5.82–5.80 (d, <i>J</i> = 8.12 Hz, 1H, 1), 4.65 (bs, 1H, 7), 4.06 (m, 1H, 2), 3.93–3.81 (m, 1H, 5'), 3.30–3.24 (m, 2H, 6), 3.06–3.00 (q, <i>J</i> = 6.59 Hz, 2H, 3), 2.04–1.95, 1.81–1.38, 1.29–1.21 (3m, 10H, 4, 5, 3', 4', 6')	157.65 (1), 151.75 (10), 150.17 (11), 148.93 (8), 133.40 (13), 127.32 (14), 124.16, 123.99 (12, 15), 117.43 (16), 98.64 (9), 70.53 (5), 48.28 (2), 42.44 (6), 42.18 (6), 38.82 (3), 33.72 (4'), 31.45 (3'), 27.81 (4), 25.18 (5')	377.1 (<i>M</i> +1) ⁺	C ₁₉ H ₂₅ ClN ₄ O ₂ (376.88)	60.55 6.69 14.87 60.69 6.61 14.90
			8.40–8.38 (d, <i>J</i> = 5.40 Hz, 1H, 10), 8.30–8.27 (d, <i>J</i> = 9.06 Hz, 1H, 15), 7.78–7.77 (d, <i>J</i> = 2.15 Hz, 1H, 12), 7.46–7.42 (dd, <i>J</i> = 2.17, 8.97 Hz, 1H, 14), 7.36–7.32 (t, <i>J</i> = 5.11 Hz, 1H, 2), 6.48– 6.46 (d, <i>J</i> = 5.48 Hz, 1H, 9), 5.94–5.90 (t, <i>J</i> = 5.57 Hz, 1H, 7), 5.75–5.72 (d, <i>J</i> = 8.49 Hz, 1H, 1'), 4.77 (bs, 1H, 6'), 4.56–4.36 (m, 2H, 4'), 3.70–3.62 (m, 1H, 2'), 3.31–3.24 (m, 4H, 6, 5'), 3.08–3.02 (q, <i>J</i> = 6.50 Hz, 2H, 3), 1.92–1.84, 1.75–1.44 (m, 6H, 4, 5, 3')	157.92 (1), 151.90 (10), 150.08 (11), 148.10 (8), 133.34 (13), 127.47 (14), 124.12, 123.97 (12, 15), 117.46 (16), 98.64 (9), 82.65–80.51 (d, <i>J</i> = 161.37 Hz, 4'), 63.67 (5'), 47.64–47.57 (d, <i>J</i> = 5.23 Hz, 2'), 42.17 (6), 38.96 (3), 32.72–32.47 (d, <i>J</i> = 19.13 Hz, 5'), 27.79 (4), 25.18 (5)	383.1 (<i>M</i> +1) ⁺	C ₁₈ H ₂₄ ClF- N ₄ O ₂ (382.86)	56.47 6.32 14.63 56.42 6.41 14.52
8	112 (decomp.)	3331, 3070, 2940, 2869, 1613, 1583, 1482, 1451, 1429, 1369, 1325, 1274, 1207, 1166, 1119, 1082, 1060, 898, 852, 806, 765, 705, 643, 597, 563, 467, 428	8.39–8.38 (d, <i>J</i> = 5.41 Hz, 1H, 10), 8.29–8.26 (d, <i>J</i> = 9.06 Hz, 1H, 15), 7.78–7.77 (d, <i>J</i> = 2.17 Hz, 1H, 12), 7.46–7.42 (dd, <i>J</i> = 2.20, 8.98 Hz, 1H, 14), 7.34–7.31 (t, <i>J</i> = 5.15 Hz, 1H, 2), 6.48– 6.45 (m, 2H, 9, 1'), 6.15–6.12 (t, <i>J</i> = 5.59 Hz, 1H, 5'), 6.07–6.03 (t, <i>J</i> = 5.77 Hz, 1H, 7), 3.95 (bs, 1H, 3'), 3.30–3.24 (m, 3H, 6, 2), 3.07–3.03 (m, 3H, 3, 2'), 1.69–1.60, 1.53–1.46 (2m, 4H, 4, 5)	158.20 (1), 151.93 (10), 150.09 (11), 149.12 (8), 133.37 (13), 130.97- 119.73 (q, <i>J</i> = 283.76 Hz, 4'), 127.25 (14), 124.12, 123.99 (12, 15), 117.47 (16), 98.66 (9), 68.84–67.71 (q, <i>J</i> = 28.35 Hz, 3'), 42.14 (6), 39.80 (2'), 38.94 (3'), 27.71 (4), 25.19 (5)	405.1 (<i>M</i> +1) ⁺	C ₁₇ H ₂₀ ClF- ₃ N ₄ O ₂ (404.81)	50.44 4.98 13.84 50.55 5.03 13.74

Compd.	M. p. (°C)	IR (KBr, film), ν_{\max} (cm ⁻¹)	NMR data (DMSO- <i>d</i> ₆ , δ , ppm)		MS (<i>m/z</i>)	Molecular formula (<i>M_r</i>)	CHN analysis, calcd./found (%)
			¹ H	¹³ C			
9	98 (decomp.)	3313, 3066, 2930, 2861, 1639, 1613, 1582, 1514, 1451, 1368, 1333, 1246, 1208, 1170, 1138, 1105, 1082, 900, 875, 853, 808, 765, 644, 529, 430	9.17 (bs, 1H, 9), 8.41-8.35 (d, <i>J</i> = 5.62 Hz, 1H, 10), 8.35-8.32 (d, <i>J</i> = 9.08 Hz, 1H, 15), 7.80-7.80 (d, <i>J</i> = 2.20 Hz, 1H, 12), 7.65-7.61 (t, <i>J</i> = 5.19 Hz, 1H, 2), 7.49-7.46 (dd, <i>J</i> = 2.23, 9.00 Hz, 1H, 14), 6.98-6.96 (d, <i>J</i> = 8.45 Hz, 2H, 5', 9'), 6.68-6.66 (d, <i>J</i> = 8.88 Hz, 2H, 6', 8'), 6.54-6.52 (d, <i>J</i> = 5.72 Hz, 1H, 9), 5.94-5.90 (t, <i>J</i> = 5.66 Hz, 7), 5.79-5.75 (t, <i>J</i> = 5.61 Hz, 1), 3.34-3.27 (q, <i>J</i> = 6.72 Hz, 2H, 2'), 3.17-3.11 (m, 2H, 6), 3.07-3.01 (q, <i>J</i> = 6.54 Hz, 2H, 3), 2.56-2.51 (m, 2H, 3'), 1.69-1.60, 1.52-1.43 (2m, 4H, 4, 5)	158.06 (1), 155.55 (7'), 150.77 (10), 150.71 (11), 147.72 (8), 133.93 (13), 129.73 (4), 129.45 (5', 7'), 126.37 (14), 124.34 (12, 15), 117.19 (16), 115.07 (6', 8'), 98.63 (9), 42.27 (6), 41.27 (2'), 38.86 (3), 35.38 (3'), 27.78 (4), 25.14 (5)	413.1 (M+1) ⁺	C ₂₂ H ₂₅ ClIN ₄ O ₂ (412.91)	63.99 6.10 64.33 6.00
			3296, 3230, 3059, 3026, 2941, 2867, 1630, 1579, 1489, 1448, 1367, 1330, 1276, 1248, 1204, 1137, 1083, 1013, 941, 897, 848, 802, 745, 697, 638, 587, 548, 512, 452	8.38-8.37 (d, <i>J</i> = 5.43 Hz, 1H, 10), 8.29-8.26 (d, <i>J</i> = 9.07 Hz, 1H, 15), 7.79-7.78 (d, <i>J</i> = 2.19 Hz, 1H, 12), 7.45-7.42 (dd, <i>J</i> = 2.22, 8.99 Hz, 1H, 14), 7.37-7.20 (m, 10H, 2, 4', 5', 7', 8', 10'-14'), 6.88-6.85 (d, <i>J</i> = 8.44 Hz, 1H, 2), 6.48-6.46 (d, <i>J</i> = 5.53 Hz, 1H, 9), 5.96-5.89 (m, 2H, 7, 1), 3.30-3.24 (q, <i>J</i> = 6.61 Hz, 2H, 6), 3.11-3.04 (q, <i>J</i> = 6.48 Hz, 2H, 3), 1.67-1.47 (m, 4H, 4, 5)	157.21 (1), 151.69 (10), 150.16 (11), 148.87 (8), 143.17 (9), 142.89 (3'), 133.43 (13), 131.23 (6'), 128.70, 128.45, 128.25, 127.30, 127.00 (4', 5', 7', 8', 10'-14'), 126.91 (14), 124.13, 124.03 (12, 15), 117.41 (16), 98.62 (9), 56.26 (2'), 42.13 (6), 38.96 (3), 27.74 (4), 25.17 (5)	493.1 (M+1) ⁺	C ₂₇ H ₂₆ Cl ₃ N ₄ O (493.43)

Table II. Drug-like properties of novel CQ-derivatives (28)

Compd.	Molecular formula	Number of atoms	M_r	$\log P$	HBD	HBA	Lipinski score ^a	MR (cm ³ mol ⁻¹)	TPSA (Å ²)
4	C ₁₈ H ₂₃ ClN ₄ O ₂	48	362.86	1.40	4	4	4	98.85	86.28
5	C ₁₉ H ₂₅ ClN ₄ O ₂	51	376.89	1.84	4	4	4	103.45	86.28
6	C ₁₉ H ₂₅ ClN ₄ O ₂	51	376.89	1.59	4	4	4	103.49	86.28
7	C ₁₈ H ₂₄ ClFN ₄ O ₂	50	382.86	1.33	4	4	4	100.88	86.28
8	C ₁₇ H ₂₀ ClF ₃ N ₄ O ₂	47	404.82	2.02	4	4	4	96.87	86.28
9	C ₂₂ H ₂₅ ClN ₄ O ₂	54	412.92	3.41	4	4	4	116.80	86.28
10	C ₂₇ H ₂₆ Cl ₂ N ₄ O	60	493.43	5.81	3	3	3	139.16	66.05

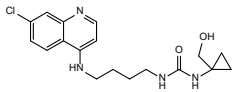
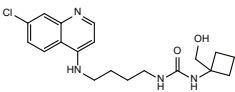
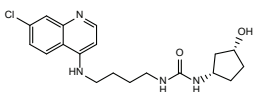
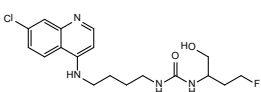
HBD – H-bond donor; HBA – H-bond acceptor; MR – molar refractivity; TPSA – topological polar surface area
^aOut of four.

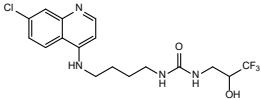
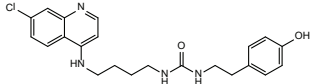
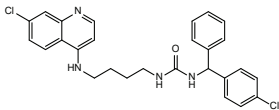
Antiproliferative activity

Antiproliferative activity was tested on four human tumor cell lines (HCT 116, MCF-7, H 460 and SW 620) utilizing a standard MTT assay. Standard anticancer drug etoposide (Eto) was used as the positive control. The results are summarized in Table III.

The results showed that chloroquine urea **9** and **10** with aromatic moieties were the most active compounds, while the ureas derived from cyclic amino alcohols (compounds

Table III. Antiproliferative activity of compounds 4–10

Compd.	Structure	IC ₅₀ (μmol L ⁻¹) ^a			
		HCT 116	MCF-7	H 460	SW 620
4		≥ 100	≥ 100	≥ 100	61 ± 26
5		37 ± 4	33 ± 8	28 ± 3	31 ± 2
6		48 ± 1	49 ± 9	54 ± 19	41 ± 4
7		≥ 100	77 ± 25	≥ 100	60 ± 27

8		35 ± 6	30 ± 8	20 ± 2	19 ± 4
9		11 ± 0.2	12 ± 2	16 ± 1	15 ± 2
10		2 ± 0.04	2 ± 0.2	2 ± 0.2	2 ± 0.01
Eto		5 ± 2	1 ± 0.7	0.1 ± 0.04	20 ± 4

Eto – etoposide; ^aIC₅₀ – the concentration that causes 50 % growth inhibition.

4–6) or aliphatic amines bearing hydroxyl group and one or three fluorine atoms (compounds 7 and 8) showed low activity or were practically inactive. Urea 10 showed activity at low micromolar concentrations, with IC₅₀ value of 2 μmol L⁻¹ towards all tested cancer cell lines, while IC₅₀ value of urea 9 was 5–8 times higher, depending on the cell line. Nevertheless, along with compound 8 it exhibited activity comparable to that of etoposide against cell line SW 620.

CONCLUSIONS

In summary, we have developed a practical and efficient route for the synthesis of chloroquine urea derivatives. The drug-likeness study showed promising bioactivity scores for the new compounds. Preliminary screening revealed that two hits, namely, 1-[4-[(7-chloroquinolin-4-yl)amino]butyl]-3-(4-hydroxyphenethyl)urea (9) and 1-[4-(4-chlorophenyl)(phenyl)methyl]-3-[4-[(7-chloroquinolin-4-yl)amino]butyl]urea (10), showed significant antiproliferative effects *in vitro* against all of the tested cancer cell lines. The differences in activity between analogues differing only in the urea region highlighted the need for further work with other substituents.

Acknowledgments. – The study was supported by the Croatian Science Foundation (research projects IP-2014-09-1501 and IP-2013-5660) and University of Zagreb (support for 2017).

Supplementary Material is available upon request.

Abbreviations, acronyms, symbols. – BtH, benzotriazole; DMEM, Dulbecco's modified Eagle's medium; Eto, etoposide; H 460, lung carcinoma cell line; HBA, H-bond acceptor; HBD, H-bond donor; HCT 116, colorectal carcinoma cell line; FBS, fetal bovine serum; IC₅₀, concentration that causes 50 % growth inhibition; log *P*, partition coefficient; MCF-7, breast adenocarcinoma cell line; MR, molar refractivity; MTT, (3-(4,5-dimethylthiazol-2-yl)-2,5-diphenyltetrazolium bromide; PDT, cell population doubling time; PG, percentage of growth; SW 620, colon carcinoma cell line; TEA, triethylamine; TPSA, topological polar surface area.

REFERENCES

1. T. L. Lemke, D. A. Williams, V. F. Roche and S. W. Zito, *Foye's Principles of Medicinal Chemistry*, 6th ed., Wolters Kluwer (Health)/Lippincott Williams & Wilkins, Philadelphia 2008.
2. E. Hempelmann, Hemozoin biocrystallization in *Plasmodium falciparum* and the antimalarial activity of crystallization inhibitors, *Parasitol. Res.* **100** (2007) 671–676; <https://doi.org/10.1007/s00436-006-0313-x>
3. C. Verbaanderd, H. Maes, M. B. Schaaf, V. P. Sukhatme, P. Pantziarka, V. Sukhatme, P. Agostinis and G. Bouche, Repurposing drugs in oncology (ReDO) – chloroquine and hydroxychloroquine as anti-cancer agents, *eCancer* **11** (2017) Article ID 781; <https://doi.org/10.3332/ecancer.2017.781>
4. H. Monma, Y. Iida, T. Moritani, T. Okimoto, R. Tanino, Y. Tajima and M. Harada, Chloroquine augments TRAIL-induced apoptosis and induces G2/M phase arrest in human pancreatic cancer cells, *PLoS One* **13** (2018) Article ID e0193990; <https://doi.org/10.1371/journal.pone.0193990>
5. V. R. Solomon and H. Lee, Chloroquine and its analogs: A new promise of an old drug for effective and safe cancer therapies, *Eur. J. Pharmacol.* **625** (2009) 220–233; <https://doi.org/10.1016/j.ejphar.2009.06.063>
6. A. K. Abdel-Aziz, S. Shouman, E. El-Demerdash, M. Elgendy and A. B. Abdel-Naim, Chloroquine as a promising adjuvant chemotherapy together with sunitinib, *Sci. Proc.* **1** (2014) Article ID e384; <https://doi.org/10.14800/sp.384>
7. F. Liu, Y. Shang and S.-Z. Chen, Chloroquine potentiates the anti-cancer effect of lidamycin on non-small cell lung cancer cells *in vitro*, *Acta Pharmacol. Sin.* **35** (2014) 645–652; <https://doi.org/10.1038/aps.2014.3>
8. A. R. Choi, J. H. Kim, Y. H. Woo, H. S. Kim and S. Yoon, Anti-malarial drugs primaquine and chloroquine have different sensitization effects with anti-mitotic drugs in resistant cancer cells, *Anticancer Res.* **36** (2016) 1641–1648.
9. A. Ganguli, D. Choudhury, S. Datta, S. Bhattacharya and G. Chakrabarti, Inhibition of autophagy by chloroquine potentiates synergistically anti-cancer property of artemisinin by promoting ROS dependent apoptosis, *Biochimie* **107** (2014) 338–349; <https://doi.org/10.1016/j.biochi.2014.10.001>
10. L. Liu, C. Han, H. Yu, W. Zhu, H. Cui, L. Zheng, C. Zhang and L. Yue, Chloroquine inhibits cell growth in human A549 lung cancer cells by blocking autophagy and inducing mitochondrial-mediated apoptosis, *Oncol. Rep.* **39** (2018) 2807–2816; <https://doi.org/10.3892/or.2018.6363>
11. F. Wang, J. Tang, P. Li, S. Si, H. Yu, X. Yang, J. Tao, Q. Lv, M. Gu, H. Yang and Z. Wang, Chloroquine enhances the radiosensitivity of bladder cancer cells by inhibiting autophagy and activating apoptosis, *Cell. Physiol. Biochem.* **45** (2018) 54–66; <https://doi.org/10.1159/000486222>
12. J. M. Mulcahy Levy, S. Zahedi, A. M. Griesinger, A. Morin, K. D. Davies, D. L. Aisner, B. K. Kleinschmidt-DeMasters, B. E. Fitzwalter, M. L. Goodall, J. Thorburn, V. Amani, A. M. Donson, D. K. Birks, D. M. Mirsky, T. C. Hankinson, M. H. Handler, A. L. Green, R. Vibhakkar, N. K. Foreman and A. Thorburn, Autophagy inhibition overcomes multiple mechanisms of resistance to BRAF inhibition in brain tumors, *eLife* **6** (2017) Article ID e19671; <https://doi.org/10.7554/eLife.19671.001>
13. T. Kimura, Y. Takabatake, A. Takahashi and Y. Isaka, Chloroquine in cancer therapy: A double-edged sword of autophagy, *Cancer Res.* **73** (2013) 3–7; <https://doi.org/10.1158/0008-5472>
14. S. Edaye, D. Tazoo, D. Scott Bohle and E. Georges, 3-Halo chloroquine derivatives overcome *Plasmodium falciparum* chloroquine resistance transporter-mediated drug resistance in *P. falciparum*, *Antimicrob. Agents Chemother.* **59** (2015) 7891–7893; <https://doi.org/10.1128/AAC.01139-15>
15. S.-J. Yeo, D.-X. Liu, H. S. Kim and H. Park, Anti-malarial effect of novel chloroquine derivatives as agents for the treatment of malaria, *Malaria J.* **16** (2017) Article ID 80 (9 pages); <https://doi.org/10.1186/s12936-017-1725-z>

16. O. M. Yvette, S. F. Malan, D. Taylor, E. Kapp and J. Joubert, Adamantane amine-linked chloroquinoline derivatives as chloroquine resistance modulating agents in *Plasmodium falciparum*, *Bioorg. Med. Chem. Lett.* **28** (2018) 1287–1291; <https://doi.org/10.1016/j.bmcl.2018.03.026>
17. E. A. Hall, J. E. Ramsey, Z. Peng, D. Hayrapetyan, V. Shkepu, B. O'Rourke, W. Geiger, K. Lam and C. F. Verschraegen, Novel organometallic chloroquine derivative inhibits tumor growth, *J. Cell. Biochem.* (2018) (in press); <https://doi.org/10.1002/jcb.26787>
18. C. Teixeira, N. Vale, B. Pérez, A. Gomes, J. R. Gomes, P. Gomes, "Recycling" classical drugs for malaria, *Chem. Rev.* **114** (2014) 11164–11220; <https://doi.org/10.1021/cr500123g>
19. V. R. Solomon, C. Hu and H. Lee, Design and synthesis of chloroquine analogs with anti-breast cancer property, *Eur. J. Med. Chem.* **45** (2010) 3916–3923; <https://doi.org/10.1016/j.ejmech.2010.05.046>
20. B. C. Pérez, I. Fernandes, N. Mateus, C. Teixeira and P. Gomes, Recycling antimalarial leads for cancer: Antiproliferative properties of *N*-cinnamoyl chloroquine analogues, *Bioorg. Med. Chem. Lett.* **23** (2013) 6769–6772; <https://doi.org/10.1016/j.bmcl.2013.10.025>
21. M. Quiliano, A. Pabón, E. Moles, L. Bonilla-Ramirez, I. Fabing, K. Y. Fong, D. A. Nieto-Aco, D. W. Wright, J. C. Pizarro, A. Vettorazzi, A. López de Cerain, E. Deharo, X. Fernández-Busquets, G. Garavito, I. Aldana and S. Galiano, Structure-activity relationship of new antimalarial 1-aryl-3-substituted propanol derivatives: Synthesis, preliminary toxicity profiling, parasite life cycle stage studies, target exploration, and targeted delivery, *Eur. J. Med. Chem.* **152** (2018) 489–514; <https://doi.org/10.1016/j.ejmech.2018.04.038>
22. F. M. Ferguson and N. S. Gray, Kinase inhibitors: the road ahead, *Nature Rev. Drug Discov.* **17** (2018) 353–377; <https://doi.org/10.1038/nrd.2018.21>
23. V. Reddy, *Organofluorine Compounds in Biology and Medicine*, 1st ed., Elsevier, Amsterdam 2015.
24. B. Meunier, A. Robert, O. Dechy-Cabaret and F. Benoit-Vical, *Dual Molecules Containing a Peroxide Derivative, Synthesis and Therapeutic Applications thereof*, U. S. Pat. 20040038957A1, 26 Feb 2004.
25. I. Kalčić, M. Zovko, M. Jadrijević-Mladar Takač, B. Zorc and I. Butula, Synthesis and reactions of some azolecarboxylic acid derivatives, *Croat. Chem. Acta* **76** (2003) 217–228.
26. Z. Rajić, D. Hadjipavlou-Litina, E. Pontiki, M. Kralj, L. Šuman and B. Zorc, The novel ketoprofen amides – Synthesis and biological evaluation as antioxidants, lipoxygenase inhibitors and cytostatic agents, *Chem. Biol. Drug. Des.* **75** (2010) 641–652; <https://doi.org/10.1111/j.1747-0285.2010.00963.x>
27. L. Uzelac, Đ. Škalamera, K. Mlinarić-Majerski, N. Basarić and M. Kralj, Selective photocytotoxicity of anthrols on cancer stem-like cells: the effect of quinone methides or reactive oxygen species, *Eur. J. Med. Chem.* **137** (2017) 558–574; <https://doi.org/10.1016/j.ejmech.2017.05.063>
28. Chemicalize, 2017, ChemAxon Ltd., Budapest, Hungary; available from <https://chemicalize.com/>